Available online at www.sciencedirect.com
ScienceDirect
Journal of Sound and Vibration 310 (2008) 1057–1079
JOURNAL OF SOUND AND VIBRATION
www.elsevier.com/locate/jsvi

Timoshenko beam-column with generalized end conditions on elastic foundation: Dynamic-stiffness matrix and load vector

Luis G. Arboleda-Monsalve[a,*,1], David G. Zapata-Medina[b], J. Darío Aristizabal-Ochoa[c]

[a]*Janssen and Spaans Engineering Inc., Indianapolis, IN 46216, USA*
[b]*Department of Civil and Environmental Engineering, Northwestern University, Evanston, IL 60208, USA*
[c]*School of Mines, National University, Colombia*

Received 25 May 2006; received in revised form 4 August 2007; accepted 20 August 2007
Available online 17 October 2007

Abstract

The dynamic-stiffness matrix and load vector of a Timoshenko beam-column resting on a two-parameter elastic foundation with generalized end conditions are presented. The proposed model includes the frequency effects on the stiffness matrix and load vector as well as the coupling effects of: (1) bending and shear deformations along the member; (2) translational and rotational lumped masses at both ends; (3) translational and rotational masses uniformly distributed along its span; (3) axial load (tension or compression) applied at both ends; and (4) shear forces along the span induced by the applied axial load as the beam deforms according to the "modified shear equation" proposed by Timoshenko. The dynamic analyses of framed structures can be performed by including the effects of the imposed frequency ($\omega > 0$) on the dynamic-stiffness matrix and load vector while the static and stability analyses can be carried out by making the frequency $\omega = 0$. The proposed model and corresponding dynamic-stiffness matrix and load vector represent a general solution capable to solve, just by using a single segment per element, the static, dynamic and stability analyses of any elastic framed structure made of prismatic beam-columns with semi-rigid connections resting on two-parameter elastic foundations. Analytical results indicate that the elastic behavior of framed structures made of beam-columns is frequency dependent and highly sensitive to the coupling effects just mentioned. Three comprehensive examples are presented to show the capacities and validity of the proposed method and the obtained results are compared with the finite element method and other analytical approaches.

1. Introduction

The static, dynamic, and stability analyses of framed structures made up of beams and beam-columns under any load conditions are of great importance in engineering. These analyses are treated in many textbooks (Refs. [1–5] among many others) using different methods (continuous, lumped, matrix analysis, FEM, BEM,

*Corresponding author. Fax: +1 317 2598262.
E-mail address: larboleda@jsengr.com (L.G. Arboleda-Monsalve).
[1]Formerly, Graduate Student, Purdue University, West Lafayette, IN, USA.

0022-460X/$ - see front matter © 2007 Elsevier Ltd. All rights reserved.
doi:10.1016/j.jsv.2007.08.014

Nomenclature

$a_o,\ldots,a_n$ coefficients of the Fourier series utilized to describe the applied transverse load
A_g gross sectional area of the beam-column
A_s effective area for shear of the beam-column ($=kA$)
A_p, B_p, C_p constants that define the particular solution of differential Eq. (15)
$b^2, R^2, s^2, D^2, F^2, \bar{Q}, \bar{x}, \bar{S}_a, \bar{S}_b, \bar{J}_a, \bar{J}_b, \bar{m}_a$, and $\bar{m}_b$ - dimensionless parameters
C_1, C_2, C_3, C_4 constants according to boundary conditions [see Eqs. (35)–(38)]
E elastic modulus of the material
$\{F_{EF}\}$ loading vector, fixed-end forces and moments in member AB due to external applied load
G shear modulus of the material
I moment of inertia of the beam-column cross section
J_a and J_b rotational inertia of the concentrated masses at A and B, respectively
k effective shear factor of the beam-column cross section
k_S and k_G two parameters of the elastic foundation [ballast modulus k_S, and transverse modulus k_G]
$[K]$ dynamic-stiffness matrix of the beam-column
L beam-column span
m_a and m_b lumped masses located at ends A and B, respectively
$\bar{m}_a$ and $\bar{m}_b$ ratios of the lumped masses located at ends A and B ($=m_a/\bar{m}L$ and $=m_b/\bar{m}L$), respectively
$\bar{m}$ mass per unit length of the beam-column
M bending moment
$\bar{M}(\bar{x})$ bending moment parameter (dimensionless)
P compression or tension axial load applied at the ends of the beam-column
$q(x, t)$ applied transverse load [$=Q(x)\sin\omega t$]
r radius of gyration of the beam cross section
R slenderness parameter ($=r/L$)
R_a and R_b stiffness indices of the flexural connections at A and B, respectively
S_a and S_b stiffness of the lateral bracings at ends A and B of the beam-column, respectively
t time
$\{U\}$ vector of displacements and rotations
V shear force
$\bar{V}(\bar{x})$ dimensionless shear force
x coordinate along the centroidal axis of the beam-column
y total lateral deflection of the centroidal axis of the beam-column
$Y(x)$ shape-function of the total lateral deflection of the centroidal axis of the beam-column
$\bar{Y}(\bar{x})$ dimensionless shape-function of the total lateral deflection of the centroidal axis
γ_s shear distortion
θ slope due to bending of the centroidal line of the beam-column
$\partial^2 y/\partial t^2$ lateral acceleration of the centroidal axis of the beam-column
$\partial^2\theta/\partial t^2$ angular acceleration of the centroidal axis of the beam-column
$\Theta(\bar{x})$ shape-function of the slope of the centroidal axis of the beam-column due to bending only
κ_a and κ_b stiffness of the flexural connections at A and B, respectively (force × distance)
μ Poisson ratio
ρ_a and ρ_b fixity factors at ends A and B of the beam-column, respectively
ω circular frequency

etc.), and different theories (Bernoulli–Euler, Rayleigh, bending and shear, Timoshenko, modified Timoshenko's theory being the most common).

Timoshenko [6,7] was the first to analyze the simultaneous coupling effects between bending and shear deformations, and between translational and rotational inertias in beams (that is why the term Timoshenko beam has been widely utilized in the technical literature). Numerous studies have been carried out to investigate these coupling effects. Cheng [8], for example, studied extensively the Timoshenko beam using continuous models and matrix methods. Cheng and Tseng [9] and Cheng and Pantelides [10] developed the dynamic matrix of the Timoshenko beam with applications to plane frames. Morfidis and Avramidis [11,12] developed a generalized beam element on a two-parameter elastic foundation with semi-rigid connections and rigid offsets. Timoshenko [6,7], Goodman and Sutherland [13], Huang [14], Hurty and Rubenstein [15]

discussed the problem of the simultaneous coupling effects of bending and shear deformations and translational and rotational inertias in the vibration of beams. Aristizabal-Ochoa [16] discussed the effects of rotational inertia, axial force, shear deformations, and concrete cracking on the natural frequencies of large-scale reinforced-concrete structural walls. Geist and McLaughlin [17] discussed the phenomenon of double frequencies in Timoshenko beams at certain values of beam slenderness (L/r). Abbas [18] presented the vibration analysis of Timoshenko beams with elastically restrained ends using the finite element method.

Kausel [19] proved that there are still some cases like the free–free and pinned–free shear beams that invalidates the classical theory of Bernoulli–Euler and the classical shear wave equation. The classic solution for the vibration of beams and beam-columns based on the Bernoulli–Euler theory (that neglects the combined effects of shear deflections and rotational inertias along the member) violates the principle of conservation of angular momentum even in slender beams. In addition, solutions obtained from methods (continuous, lumped, matrix analysis, FEM, etc.), based on bending deformations only (i.e., neglecting the combined effects of shear deflections and rotational inertias along the member) overestimate all natural frequencies of short beams and the natural frequencies of the higher modes of slender beams as described by Weaver et al. [4]. Aristizabal-Ochoa [20] presented the complete free vibration analysis of the Timoshenko beam-column with generalized end conditions including the phenomenon of inversion of vibration modes (i.e. higher modes crossing lower modes) in shear beams with pinned–free and free–free end conditions, and also the phenomenon of double frequencies at certain values of beam slenderness (L/r). Areiza-Hurtado et al. [21], presented the static second-order stiffness matrix of beam-columns on a first-order elastic foundation which is a particular case of the present study when the second-parameter of elastic foundation and the circular frequency are set to zero.

As a consequence, there is a real need for a general matrix approach by which the static, dynamic, and stability response of framed structures made up of beam-columns with any end conditions and supported on elastic soils can be determined directly. The main objective of this publication is to derive the dynamic-stiffness matrix and load vector of a Timoshenko beam-column resting on a two-parameter elastic foundation with generalized end conditions. The proposed model includes the frequency effects on the stiffness matrix and load vector as well as the coupling effects of: (1) bending and shear deformations along the member; (2) translational and rotational lumped masses at both ends; (3) translational and rotational masses uniformly distributed along its span; (4) axial load (tension or compression) applied at both ends; and (5) shear forces along the span induced by the applied axial load as the beam-column deforms according to the ''modified shear equation'' proposed by Timoshenko. The dynamic-stiffness matrix and load vector are programmed using classic matrix methods to study the static, dynamic and stability behavior of framed structures made up of beam-columns resting on two-parameter elastic foundations with semi-rigid end connections. Three comprehensive examples are presented to show the capacities and validity of the proposed method.

2. Structural model

The proposed beam-column model is an extension of that presented by Aristizabal-Ochoa [20] including the effects of a two-parameter elastic foundation defined by the ballast modulus k_S and the transverse modulus k_G [22], and an applied external transverse load $q(x, t)$ as shown in Fig. 1. The element is made of the beam-column itself AB, the end flexural connections κ_a and κ_b (whose dimensions are given in force × distance/radian), and the lateral springs or bracings S_a and S_b (whose dimensions are given in force/distance) at A and B, respectively.

The ratios $R_a = \kappa_a/(EI/L)$ and $R_b = \kappa_b/(EI/L)$ are denoted as the *bending stiffness indices* of the flexural connections at ends A and B, respectively. In addition, the ratios $\bar{S}_a = S_a/(A_sG/L)$ and $\bar{S}_b = S_b/(A_sG/L)$ are denoted as the *shear stiffness indices* of the transverse connections at ends A and B, respectively. Both indices $R_{a,b}$ and $\bar{S}_{a,b}$ allow to the analyst to simulate any end support condition applied to the beam-column. For convenience the following two terms ρ_a and ρ_b [23,24] denoted as the *fixity factors* at A and B, respectively, are utilized: $\rho_a = 1/(1 + 3/R_a)$, and $\rho_b = 1/(1 + 3/R_b)$.

It is assumed that the beam-column AB: (1) is made of a homogenous linear elastic material with moduli E and G; (2) its centroidal axis is a straight line; (3) is loaded axially at the ends along its centroidal axis x with a constant load P, and transversally along the span with an applied external transverse load $q(x, t)$; (4) its

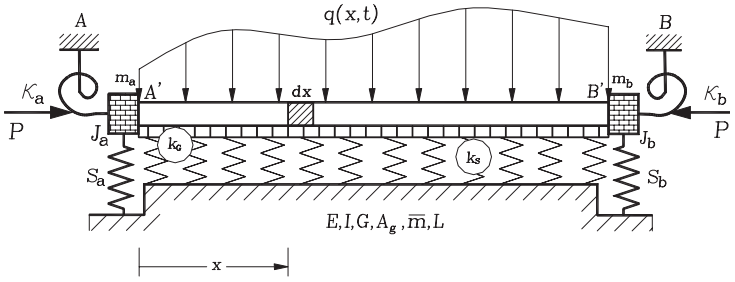

Fig. 1. Structural model.

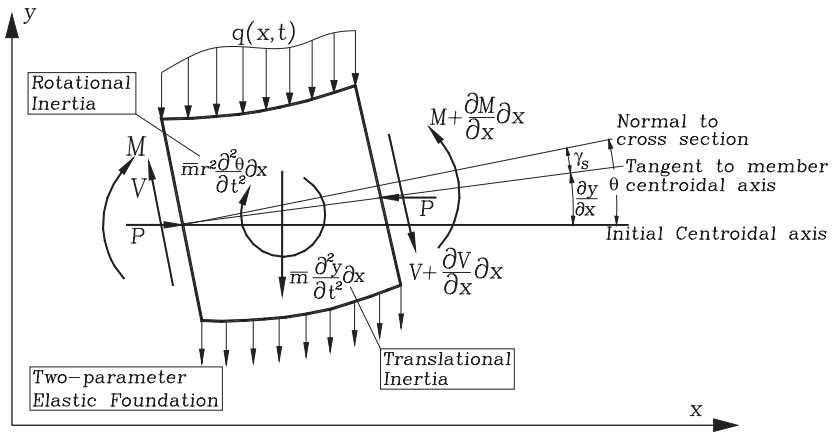

Fig. 2. Forces, moments, and deformations on the differential element.

transverse cross section is doubly symmetric (i.e., its centroid coincides with the shear center) with a gross area A_g, an effective shear area $A_s = kA_g$, and a principal moment of inertia $I = A_g r^2$ about the plane of bending; (5) has uniform mass per unit length $\bar{m}$; (6) has two lumped masses attached at the extremes A and B of magnitude m_a and m_b and rotational moments of inertia J_a and J_b, respectively; and (7) all transverse deflections, rotations, and strains along the beam are small so that the principle of superposition is applicable.

3. Governing equations and general solution

The dynamic-stiffness matrix and loading vector of the beam-column just described above (Fig. 1) are derived by applying the basic concepts of dynamic equilibrium on the differential element shown in Fig. 2 and compatibility conditions at the ends of the member. The transverse and rotational equilibrium equations are:

$$\frac{\partial V}{\partial x} = -\bar{m}\frac{\partial^2 y}{\partial t^2} - k_S y + k_G \frac{\partial^2 y}{\partial x^2} - q(x,t) \tag{1}$$

and

$$\frac{\partial M}{\partial x} = V + \bar{m}r^2\frac{\partial^2 \theta}{\partial t^2} - P\frac{\partial y}{\partial x}. \tag{2}$$

From Fig. 2, the shear distortion can be expressed as

$$\gamma_s = \theta - \frac{\partial y}{\partial x} \tag{3}$$

and according to the "modified shear approach" proposed by Timoshenko and Gere [1], the applied axial force P induces a shear component equal to $P \sin\theta \approx P\theta$. Then, the total shear across the section becomes $V-P\theta$. Thus, the shear force equation is

$$V = A_s G\left(\theta - \frac{\partial y}{\partial x}\right) + P\theta \tag{4}$$

and the bending moment equation is

$$M = EI\frac{\partial \theta}{\partial x}. \tag{5}$$

Substituting Eqs. (4) and (5) into Eqs. (1) and (2),

$$A_s G\left(\frac{\partial \theta}{\partial x} - \frac{\partial^2 y}{\partial x^2}\right) + P\frac{\partial \theta}{\partial x} = -\bar{m}\frac{\partial^2 y}{\partial t^2} - k_S y + k_G\frac{\partial^2 y}{\partial x^2} - q(x,t), \tag{6}$$

$$EI\frac{\partial^2 \theta}{\partial x^2} = A_s G\left(\theta - \frac{\partial y}{\partial x}\right) + P\theta + \bar{m}r^2\frac{\partial^2 \theta}{\partial t^2} - P\frac{\partial y}{\partial x}, \tag{7}$$

applying separation of variables to the functions $y(x, t)$, $\theta(x, t)$ and $q(x, t)$:

$$y(x,t) = Y(x)\sin(\omega t), \tag{8}$$

$$\theta(x,t) = \Theta(x)\sin(\omega t), \tag{9}$$

$$q(x,t) = Q(x)\sin(\omega t) \tag{10}$$

and substituting into Eqs. (6) and (7), the following expressions are obtained:

$$(A_s G + P)\frac{\mathrm{d}\Theta}{\mathrm{d}x} - (A_s G + k_G)\frac{\mathrm{d}^2 Y}{\mathrm{d}x^2} + (k_S - \bar{m}\omega^2)Y + Q(x) = 0, \tag{11}$$

$$EI\frac{\mathrm{d}^2\Theta}{\mathrm{d}x^2} - (A_s G + P - \bar{m}r^2\omega^2)\Theta + (A_s G + P)\frac{\mathrm{d}Y}{\mathrm{d}x} = 0. \tag{12}$$

Eqs. (11) and (12) represent the vertical and rotational dynamic equilibrium of the beam-column shown in Fig. 1. These equations, which govern the elastic dynamic behavior of the beam-column, are second-order differential equations coupled in Y and Θ.

Notice that the vertical (or transverse) equilibrium represented by Eq. (11) apparently is not affected by the rotational inertia $\bar{m}r^2$. This feature is used by most analysts in the classical solutions of the flexural beam (Bernoulli's theory) and shear beam (shear wave equation), violating the principle of conservation of angular momentum as demonstrated by Kausel [19]. However, when the coupling effects between the bending and shear deformations and also between the translational and rotational inertias along the beam are taken into consideration, like the Timoshenko beam-column with generalized end conditions presented by Aristizabal-Ochoa [20], the principle of conservation of angular momentum is fulfilled. As previously stated, this model is capable to reproduce, as a special case, the non-classical modes of shear beams reported by Kausel [19], including the phenomenon of inversion of vibration modes (i.e. higher modes crossing lower modes) in shear beams with pinned–free and free–free end conditions, and also the phenomenon of double frequencies at certain values of r/L for the beam.

Also, notice that when the shear deformations are neglected (i.e., when $\gamma_s = 0$ or $\theta = \partial y/\partial x$), any transverse section of the member remains normal to the centroidal axis, and consequently Eqs. (11) and (12) become uncoupled if the applied axial load P is zero. However, when the simultaneous effects of shear deformations and axial load are taken into account, both the transverse deformation (y) and the slope of the centroidal axis ($\partial y/\partial x$) increase. As a result, the shape-functions $Y(x)$ and $\Theta(x)$ of the transverse deflection and rotation of any section become coupled making the solution more complex, particularly when the support conditions are generalized, as it is considered in this publication.

To facilitate the static, dynamic, and stability analyses of Timoshenko beam-columns supported on two-parameter elastic foundation, which depend on 20 parameters (E, G, L, r, A_g, A_s, k_S, k_G, P, Q, $\bar{m}$, ω, κ_a, κ_b, S_a, S_b, m_a, m_b, J_a, and J_b), the non-dimensional terms presented in Table 1 are introduced into Eqs. (11) and (12):

$$(1+F^2s^2)\frac{\mathrm{d}\Theta}{\mathrm{d}\bar{x}} - (1+D_G^2s^2)\frac{\mathrm{d}^2\bar{Y}}{\mathrm{d}\bar{x}^2} + (D_S^2s^2 - b^2s^2)\bar{Y} + \bar{Q}(\bar{x}) = 0, \tag{13}$$

$$s^2\frac{\mathrm{d}^2\Theta}{\mathrm{d}\bar{x}^2} - (1+F^2s^2 - b^2s^2R^2)\Theta + (1+F^2s^2)\frac{\mathrm{d}\bar{Y}}{\mathrm{d}\bar{x}} = 0, \tag{14}$$

where $\bar{x} = x/L$ and $\bar{Y} = Y/L$. The complete differential equation for the dynamic equilibrium of a prismatic beam-column is obtained by eliminating Θ from Eqs. (13) and (14), as follows:

$$\frac{\mathrm{d}^4\bar{Y}}{\mathrm{d}\bar{x}^4} + 2\Omega\frac{\mathrm{d}^2\bar{Y}}{\mathrm{d}\bar{x}^2} + \varepsilon\bar{Y} = \frac{b^2R^2s^2 - 1 - F^2s^2}{s^2(1+D_G^2s^2)}\bar{Q}(\bar{x}) + \frac{1}{(1+D_G^2s^2)}\frac{\mathrm{d}^2\bar{Q}(\bar{x})}{\mathrm{d}\bar{x}^2}, \tag{15}$$

where

$$\Omega = \frac{b^2s^2 - D_S^2s^2 + b^2R^2 + F^2 + F^4s^2 + b^2s^2R^2D_G^2 - D_G^2 - F^2s^2D_G^2}{2(1+D_G^2s^2)} \tag{16}$$

and

$$\varepsilon = \frac{b^4R^2s^2 - b^2D_S^2R^2s^2 - b^2 + D_S^2 - b^2F^2s^2 + D_S^2F^2s^2}{1+D_G^2s^2}. \tag{17}$$

Table 1
Dimensionless parameters

Parameter	Description
$b^2 = \dfrac{\bar{m}\omega^2}{EI/L^4}$	Frequency parameter
$s^2 = \dfrac{EI/L^2}{A_sG}$	Bending-to-shear stiffness parameter
$F^2 = \dfrac{P}{EI/L^2}$	Axial-load parameter
$R^2 = \dfrac{r^2}{L^2}$	Slenderness parameter
$D_S^2 = \dfrac{k_S}{EI/L^4}$	First-parameter of the elastic foundation
$D_G^2 = \dfrac{k_G}{EI/L^2}$	Second-parameter of the elastic foundation
$\bar{Q}(\bar{x}) = \dfrac{Q(\bar{x})}{A_sG/L}$	Applied transverse load parameter
$\bar{V}_a = \dfrac{V_a}{A_sG}$ and $\bar{V}_b = \dfrac{V_b}{A_sG}$	End-shear force parameters
$\bar{M}_a = \dfrac{M_a}{EI/L}$ and $\bar{M}_b = \dfrac{M_b}{EI/L}$	End bending-moment parameters
$R_a = \dfrac{\kappa_a}{EI/L}$ and $R_b = \dfrac{\kappa_b}{EI/L}$	End flexural-connection indices
$\bar{S}_a = \dfrac{S_a}{A_sG/L}$ and $\bar{S}_b = \dfrac{S_b}{A_sG/L}$	End bracing indices
$\bar{m}_a = \dfrac{m_a}{\bar{m}L}$ and $\bar{m}_b = \dfrac{m_b}{\bar{m}L}$	End mass indices
$\bar{J}_a = \dfrac{J_a}{\bar{m}L^3}$ and $\bar{J}_b = \dfrac{J_b}{\bar{m}L^3}$	End rotational-mass indices

The complete solution to Eq. (15), which is a fourth-order non-homogeneous linear differential equation with constant coefficients, is made up of the *homogeneous* and the *particular* solutions as follows:

$$\bar{Y}(\bar{x}) = \bar{Y}_H(\bar{x}) + \bar{Y}_P(\bar{x}), \tag{18}$$

where the form of the homogeneous solution is: $\bar{Y}_H = c\,e^{m\bar{x}}$. After substituting into Eq. (15), the following polynomial is obtained: $m^4 + 2\Omega m^2 + \varepsilon = 0$, whose solutions are $m^2 = -\Omega \pm \sqrt{\Omega^2 - \varepsilon}$ or $m = \pm i\beta, \pm\alpha$, where

$$\beta = \sqrt{\Omega + \sqrt{\Omega^2 - \varepsilon}} \tag{19}$$

and

$$\alpha = \sqrt{-\Omega + \sqrt{\Omega^2 - \varepsilon}}, \tag{20}$$

thus, the homogeneous solution is

$$\bar{Y}_H = C_1 \sin(\beta\bar{x}) + C_2 \cos(\beta\bar{x}) + C_3 \sinh(\alpha\bar{x}) + C_4 \cosh(\alpha\bar{x}). \tag{21}$$

Note: If $\varepsilon > 0$ the following changes must be made in Eq. (21): α for $i\alpha$; $\sin\alpha$ for $\sinh\alpha$; and $\cos\alpha$ for $\cosh\alpha$ (where $i = \sqrt{-1}$). These solutions are identical to those presented by Karnovsky and Lebed [25].

The particular solution that corresponds to the applied load and its second derivative [see Eq. (15)] is better expressed in terms of a Fourier series as in Eq. (A.7) (see Appendix A).

After substituting Eq. (A.7) into Eq. (15), the particular solution is obtained:

$$\bar{Y}_p = A_p + \sum_{n=1}^{\infty} B_p \cos(n\pi\bar{x}), \tag{22}$$

where

$$A_p = \frac{A_o}{\varepsilon} \frac{(b^2R^2s^2 - F^2s^2 - 1)}{s^2(1 + D_G^2 s^2)} \tag{23}$$

and

$$B_p = \frac{A_n[b^2R^2s^2 - F^2s^2 - s^2(n\pi)^2 - 1]}{s^2(1 + D_G^2 s^2)[\varepsilon - 2\Omega(n\pi)^2 + (n\pi)^4]}. \tag{24}$$

Finally, adding up Eqs. (21) and (22) the total lateral deflection becomes:

$$\bar{Y}(\bar{x}) = C_1 \sin(\beta\bar{x}) + C_2 \cos(\beta\bar{x}) + C_3 \sinh(\alpha\bar{x}) + C_4 \cosh(\alpha\bar{x}) + A_p + \sum_{n=1}^{\infty} B_p \cos(n\pi\bar{x}). \tag{25}$$

The solution for Θ can be obtained by differentiating Eq. (13) and substituting $d\bar{Y}/d\bar{x}$ from Eq. (14) and its derivatives, to obtain the following differential equation in terms of Θ:

$$\frac{d^4\Theta}{d\bar{x}^4} + 2\Omega\frac{d^2\Theta}{d\bar{x}^2} + \varepsilon\Theta = -\frac{1 + F^2s^2}{s^2(1 + D_G^2 s^2)} \frac{d\bar{Q}(\bar{x})}{d\bar{x}}, \tag{26}$$

where Ω and ε are given by Eqs. (16) and (17).

The complete solution to Eq. (26), which is again a fourth-order non-homogeneous linear differential equation with constant coefficients, is as follows:

$$\Theta(\bar{x}) = C_1' \sin(\beta\bar{x}) + C_2' \cos(\beta\bar{x}) + C_3' \sinh(\alpha\bar{x}) + C_4' \cosh(\alpha\bar{x}) + \sum_{n=1}^{\infty} C_p \sin(n\pi\bar{x}), \tag{27}$$

where the relationships between constants C_1, C_2, C_3, C_4, and C_1', C_2', C_3', C_4' are given by the following expressions:

$$C_1' = -C_2\lambda, \tag{28}$$

$$C_2' = C_1\lambda, \tag{29}$$

$$C_3' = C_4\delta, \tag{30}$$

$$C_4' = C_3\delta, \tag{31}$$

where

$$\lambda = \frac{\beta^2(1 + D_G^2 s^2) - b^2 s^2 + D_S^2 s^2}{(1 + F^2 s^2)\beta}, \tag{32}$$

$$\delta = \frac{\alpha^2(1 + D_G^2 s^2) + b^2 s^2 - D_S^2 s^2}{(1 + F^2 s^2)\alpha} \tag{33}$$

and

$$C_p = \frac{B_p[b^2 s^2 - D_S^2 s^2 - (1 + D_G^2 s^2)(n\pi)^2] - A_n}{n\pi(1 + F^2 s^2)}. \tag{34}$$

3.1. Shears, moments, deflections and rotations at the ends

In order to determine the stiffness matrix and load vector, the conditions at ends A and B of the beam-column are evaluated following the sign convention for forces, moments, rotations and transverse deflections shown in Fig. 3, as follows:
at $\bar{x} = 0$:

$$\bar{V}_a = (\bar{S}_a - \bar{m}_a b^2 s^2)\,\bar{Y}(0) + (1 + F^2 s^2)\Theta(0) - (1 + D_G^2 s^2)\frac{\mathrm{d}\bar{Y}(0)}{\mathrm{d}\bar{x}}, \tag{35}$$

$$\bar{M}_a = -\bar{J}_a b^2 \Theta(0) - \frac{\mathrm{d}\Theta(0)}{\mathrm{d}\bar{x}} \tag{36}$$

and at $\bar{x} = 1$:

$$\bar{V}_b = (\bar{S}_b - \bar{m}_b b^2 s^2)\,\bar{Y}(1) - (1 + F^2 s^2)\Theta(1) + (1 + D_G^2 s^2)\frac{\mathrm{d}\bar{Y}(1)}{\mathrm{d}\bar{x}}, \tag{37}$$

$$\bar{M}_b = -\bar{J}_b b^2 \Theta(1) + \frac{\mathrm{d}\Theta(1)}{\mathrm{d}\bar{x}}. \tag{38}$$

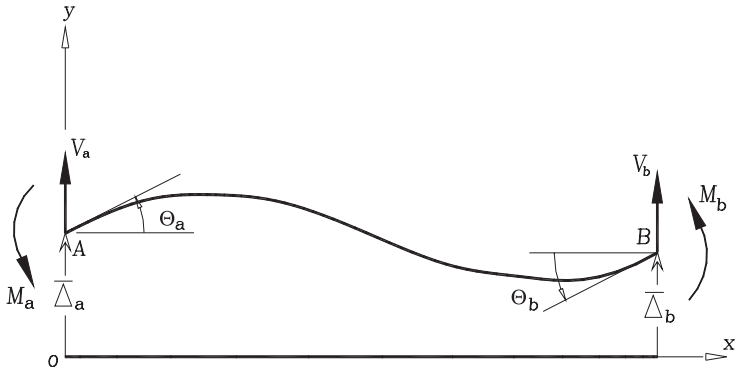

Fig. 3. Sign convention (deflections, rotations, shear forces and moments).

Eqs. (35)–(38) can be expressed in matrix form as follows:

$$\{\bar{M}\} = [S]\{C\} + \{J\}, \tag{39}$$

where

$$\{\bar{M}\} = \begin{Bmatrix} \bar{V}_a \\ \bar{M}_a \\ \bar{V}_b \\ \bar{M}_b \end{Bmatrix}, \tag{40}$$

$$\{C\} = \begin{Bmatrix} C_1 \\ C_2 \\ C_3 \\ C_4 \end{Bmatrix}, \tag{41}$$

$$\{J\} = \begin{Bmatrix} \left(\bar{S}_a - \bar{m}_a b^2 s^2\right)\left(A_p + \sum_{n=1}^{\infty} B_P\right) \\ -\sum_{n=1}^{\infty} C_P(n\pi) \\ \left(\bar{S}_b - \bar{m}_b b^2 s^2\right)\left(A_p + \sum_{n=1}^{\infty} B_P \cos(n\pi)\right) \\ \sum_{n=1}^{\infty} C_P(n\pi)\cos(n\pi) \end{Bmatrix} \tag{42}$$

and

$$[S] = \begin{bmatrix} S_{11} & S_{12} & S_{13} & S_{14} \\ S_{21} & S_{22} & S_{23} & S_{24} \\ S_{31} & S_{32} & S_{33} & S_{34} \\ S_{41} & S_{42} & S_{43} & S_{44} \end{bmatrix} \tag{43}$$

in which:

$$\begin{aligned}
&S_{11} = (1 + F^2 s^2)\lambda - \beta(1 + D_G^2 s^2);\ S_{12} = \bar{S}_a - \bar{m}_a b^2 s^2, \\
&S_{13} = (1 + F^2 s^2)\delta - \alpha(1 + D_G^2 s^2) S_{14} = \bar{S}_a - \bar{m}_a b^2 s^2, \\
&S_{21} = -\bar{J}_a b^2 \lambda, \quad S_{22} = \lambda\beta, \quad S_{23} = -\bar{J}_a b^2 \delta, \quad S_{24} = -\delta\alpha, \\
&S_{31} = \left(\bar{S}_b - \bar{m}_b b^2 s^2\right)\sin\beta - (1 + F^2 s^2)\lambda\cos\beta + (1 + D_G^2 s^2)\beta\cos\beta, \\
&S_{32} = \left(\bar{S}_b - \bar{m}_b b^2 s^2\right)\cos\beta + (1 + F^2 s^2)\lambda\sin\beta - (1 + D_G^2 s^2)\beta\sin\beta, \\
&S_{33} = \left(\bar{S}_b - \bar{m}_b b^2 s^2\right)\sinh\alpha - (1 + F^2 s^2)\delta\cosh\alpha + (1 + D_G^2 s^2)\alpha\cosh\alpha, \\
&S_{34} = \left(\bar{S}_b - \bar{m}_b b^2 s^2\right)\cosh\alpha - (1 + F^2 s^2)\delta\sinh\alpha + (1 + D_G^2 s^2)\alpha\sinh\alpha, \\
&S_{41} = -\bar{J}_b b^2 \lambda\cos\beta - \lambda\beta\sin\beta, \quad S_{42} = \bar{J}_b b^2 \lambda\sin\beta - \lambda\beta\cos\beta, \\
&S_{43} = -\bar{J}_b b^2 \delta\cosh\alpha + \delta\alpha\sinh\alpha, \quad \text{and} \quad S_{44} = -\bar{J}_b b^2 \delta\sinh\alpha + \delta\alpha\cosh\alpha.
\end{aligned}$$

Likewise, the displacements and rotations at A and B are:
at $\bar{x} = 0$:

$$\bar{\Delta}_a = \bar{Y}(0), \tag{44}$$

$$\rho_a \Theta_a = \rho_a \Theta(0) + \frac{(1-\rho_a)}{3}\bar{M}_a \tag{45}$$

and at $\bar{x} = 1$:

$$\bar{\Delta}_b = \bar{Y}(1), \tag{46}$$

$$\rho_b \Theta_b = \rho_b \Theta(1) + \frac{(1-\rho_b)}{3}\bar{M}_b. \tag{47}$$

Eqs. (44)–(47) can be expressed in matrix form as follows:

$$[H]\{U\} = [Z]\{C\} + [B]\{\bar{M}\} + \{N\}, \tag{48}$$

where

$$[H] = \begin{bmatrix} 1 & 0 & 0 & 0 \\ 0 & \rho_a & 0 & 0 \\ 0 & 0 & 1 & 0 \\ 0 & 0 & 0 & \rho_b \end{bmatrix}, \tag{49}$$

$$[B] = \begin{bmatrix} 0 & 0 & 0 & 0 \\ 0 & \dfrac{1-\rho_a}{3} & 0 & 0 \\ 0 & 0 & 0 & 0 \\ 0 & 0 & 0 & \dfrac{1-\rho_b}{3} \end{bmatrix}, \tag{50}$$

$$\{U\} = \begin{Bmatrix} \bar{\Delta}_a \\ \Theta_a \\ \bar{\Delta}_b \\ \Theta_b \end{Bmatrix}, \tag{51}$$

$$\{N\} = \begin{Bmatrix} A_P + \sum_{n=1}^{\infty} B_P \\ 0 \\ A_P + \sum_{n=1}^{\infty} B_P \cos(n\pi) \\ 0 \end{Bmatrix} \tag{52}$$

and

$$[Z] = \begin{bmatrix} 0 & 1 & 0 & 1 \\ \rho_a\lambda & 0 & \rho_a\delta & 0 \\ \sin\beta & \cos\beta & \sinh\alpha & \cosh\alpha \\ \rho_b\lambda\cos\beta & -\rho_b\lambda\sin\beta & \rho_b\delta\cosh\alpha & \rho_b\delta\sinh\alpha \end{bmatrix}. \tag{53}$$

The set of Eqs. (35)–(38) and Eqs. (44)–(47) represent the boundary conditions of the element by itself and the compatibility conditions, respectively. These are necessary for the connectivity of members in frames and continuous beams. The second-parameter of elastic foundation is shown in the boundary conditions given by Eqs. (35)–(38) to consider the transverse modulus k_G of the nearby soil. The spring constants S_a and S_b (and its dimensionless parameters $\bar{S}_a$ and $\bar{S}_b$, respectively) can be used to represent either a foundation constant (e.g., settlement of foundation) or a lateral bracing of a beam-column element.

From Eq. (39), $\{C\}$ can be found as

$$\{C\} = [S]^{-1}\{\bar{M}\} - [S]^{-1}\{J\} \tag{54}$$

and substituting $\{C\}$ into Eq. (48), the vector of forces $\{M\}$ is

$$\{\bar{M}\} = [ZS^{-1} + B]^{-1}[H]\{U\} + [ZS^{-1} + B]^{-1}\{ZS^{-1}J - N\}. \tag{55}$$

3.2. Dynamic-stiffness matrix and load vector

The following reduced expression: $\{\bar{M}\} = [ZS^{-1} + B]^{-1}[H]\{U\}$ is obtained when the transverse load is made zero [i.e. $q(x, t) = 0$] in Eq. (55), thus:

$$[K] = [ZS^{-1} + B]^{-1}[H]. \tag{56}$$

Notice that the square matrix $[K]$ is the *dynamic-stiffness matrix* of the beam-column AB of Fig. 1, since it relates the vector of end moments and shears $\{\bar{M}\}$ with the vector of end rotations and displacements $\{U\}$. The dynamic-stiffness matrix $[K]$ depends on the following input values: E, G, L, r, A_g, A_s, k_S, k_G, P, Q, $\bar{m}$, ω, κ_a, κ_b, S_a, S_b, m_a, m_b, J_a, and J_b.

The load vector of the member AB consists of the equivalent bending moments and transverse shears applied at the ends A and B such that the end rotations and displacements become zero. Thus, the load vector obtained from Eq. (55) making $\{U\} = \{0\}$ is as follows:

$$\{F_{\mathrm{EF}}\} = [ZS^{-1} + B]^{-1}\{ZS^{-1}J - N\} \tag{57}$$

and Eq. (55) can be expressed as

$$\{\bar{M}\} = [K]\{U\} + \{F_{\mathrm{EF}}\}. \tag{58}$$

Notice that Eq. (58) is made up of the homogeneous solution $[K]\{U\}$ and the particular solution $\{F_{\mathrm{EF}}\}$. The complete solution to the beam-column of Fig. 1 includes the effects of: (a) end axial load P (tension or compression); (b) uniformly distributed translational and rotational masses along the member; (c) translational and rotational masses concentrated at the member's ends; (d) uniformly distributed two-parameter elastic foundation; (e) bending and shear deformations along the member; (f) generalized boundary conditions (i.e., flexural and transverse connections at the ends of the member); and (g) generalized transverse load. Appendix A presents the loading vector for the general case of trapezoidal load which is capable to simulate the following particular cases: uniformly distributed load, triangular load as well as concentrated force and moment.

3.3. Deflections, rotations, shears and bending moments along the member (dimensionless)

Once the end reactions are known, the lateral deflection $\bar{Y}(\bar{x})$, total rotation $\Theta(x)$, shear $\overline{V}(\bar{x})$ and moment $\bar{M}(\bar{x})$ along the beam-column between $0 \leqslant x \leqslant L$ can be calculated directly using the following equations:

$$\bar{Y}(\bar{x}) = C_1 \sin(\beta\bar{x}) + C_2 \cos(\beta\bar{x}) + C_3 \sinh(\alpha\bar{x}) + C_4 \cosh(\alpha\bar{x}) + A_p + \sum_{n=1}^{\infty} B_p \cos(n\pi\bar{x}), \tag{59}$$

$$\Theta(\bar{x}) = \lambda C_1 \cos(\beta\bar{x}) - \lambda C_2 \sin(\beta\bar{x}) + \delta C_3 \cosh(\alpha\bar{x}) + \delta C_4 \sinh(\alpha\bar{x}) + \sum_{n=1}^{\infty} C_p \sin(n\pi\bar{x}), \tag{60}$$

$$\begin{aligned}\bar{V}(\bar{x}) = {} & \phi C_1 \cos(\beta\bar{x}) - \phi C_2 \sin(\beta\bar{x}) + \psi C_3 \cosh(\alpha\bar{x}) + \psi C_4 \sinh(\alpha\bar{x}) \\ & + \sum_{n=1}^{\infty} [B_p(n\pi) + (1 + F^2 s^2) C_p] \sin(n\pi\bar{x}),\end{aligned} \tag{61}$$

$$\bar{M}(\bar{x}) = -\lambda\beta C_1 \sin(\beta\bar{x}) - \lambda\beta C_2 \cos(\beta\bar{x}) + \delta\alpha C_3 \sinh(\alpha\bar{x}) + \delta\alpha C_4 \cosh(\alpha\bar{x}) + \sum_{n=1}^{\infty} C_p(n\pi) \cos(n\pi\bar{x}), \tag{62}$$

where

$$\phi = (1 + F^2 s^2)\lambda - \beta \tag{63}$$

and

$$\psi = (1 + F^2 s^2)\delta - \alpha. \tag{64}$$

3.4. Evaluation of the ballast modulus k_S and the transverse modulus k_G

In order to determine the supporting soil parameters k_S and k_G, Vlasov and Leontiev [26] proposed the following two expressions for rectangular beams:

$$k_S = \frac{E_o b_f}{2(1-\mu_o^2)} \frac{\gamma}{A}, \tag{65}$$

$$k_G = \frac{E_o b_f}{4(1+\mu_o)} \frac{A}{\gamma}, \tag{66}$$

where

$$A = \sqrt[3]{\frac{2Eb_f h^3(1-\mu_o^2)}{12(1-\mu^2)E_o b_f}}, \quad E_o = \frac{E_s}{1-\mu_s^2}, \quad \text{and} \quad \mu_o = \frac{\mu_s}{1-\mu_s}.$$

Zhaohua and Cook [27] defined γ as a variable of the foundation properties (a common practice is to assume this value equal to 1). E and μ are the elastic modulus and the Poisson ratio of the beam-column; E_s and μ_s are those of the supporting soil; and b_f and h are the width and depth of the rectangular cross section. The second-parameter of elastic foundation models an incompressible soil layer that resists only transverse deformations and introduces shear interaction between the elements of the Winkler foundation.

Eqs. (65) and (66) were also utilized by Zhaohua and Cook [27] in the static analysis of rectangular beams on two-parameter elastic soils.

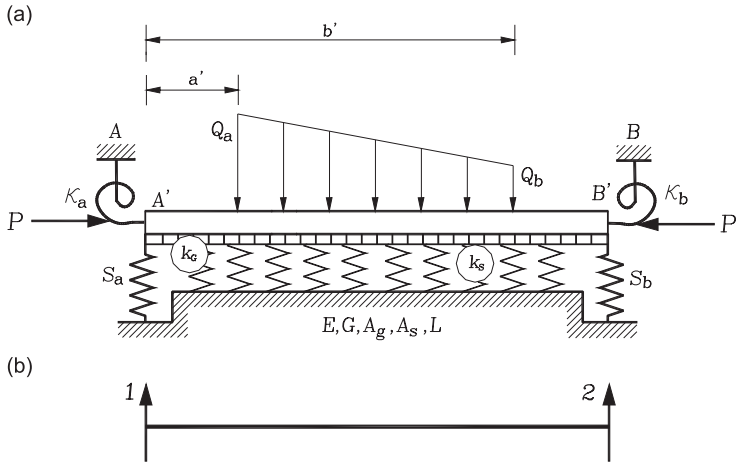

Fig. 4. Example 1: (a) beam-column under trapezoidal load; and (b) degrees of freedom.

Table 2
Parameters k_S and k_G of the elastic foundation of example 1

Soil type	Modulus of elasticity (kN/mm^2)	Poisson ratio, μ_S	k_S (kN/mm^2)	k_G (kN)
Dense sand	39.30	0.38	0.0120	5425.19
Sand and gravel	120.75	0.25	0.0298	14,680.94
Medium clay	31.05	0.35	0.0072	4989.08

4. Comprehensive examples and verification

4.1. Analysis of a beam-column resting on a two-parameter elastic foundation

For the rectangular beam-column resting on a two-parameter elastic foundation shown in Fig. 4, with E_s and μ_s of the supporting soil as suggested by Das [28], and k_S and k_G calculated using Eqs. (65) and (66) (see properties listed in Table 2), and assuming that: $E = 12\,\text{kN/mm}^2$ (12,000 MPa); $G = 5\,\text{kN/mm}^2$ (5000 MPa); $A_g = 2.5 \times 10^5\,\text{mm}^2$ (0.25 m^2); $A_s = 2.075 \times 10^5\,\text{mm}^2$ (0.2075 m^2); $I = 5.208 \times 10^9\,\text{mm}^4$ (5.208×10^{-3} m^4); $\bar{m} = 6 \times 10^7\,\text{Gg/mm}$ (600 kg/m); $L = 6000\,\text{mm}$ (6 m); $\rho_a = 0.7$; $\rho_b = 0.3$; $S_a = 15\,\text{kN/mm}$ (15,000 kN/m); $S_b = 25\,\text{kN/mm}$ (25,000 kN/m); $Q_a = 0.4\,\text{kN/mm}$ (400 kN/m); $Q_b = 0.2\,\text{kN/mm}$ (200 kN/m); $a' = 1500\,\text{mm}$ (1.5 m); $b' = 5000\,\text{mm}$ (5 m); and $P = 3000\,\text{kN}$ (compression), determine:

(I) The static stiffness matrix and the loading vector of the beam-column as well as the vertical deflections, rotations, shears and bending moments along the member. Study the effects of the transverse modulus k_G and compare the calculated results with those presented by Areiza-Hurtado et al. [21] [for the case of dense sand: $k_S = 0.012\,(\text{kN/mm}^2)$ and $k_G = 0$], and
(II) The natural frequencies of vibration of the beam-column. Study the effects of the frequency (ω) of applied dynamic trapezoidal load on the fixed-end moment at A.

Solution:

(I) *Static analysis*: The calculated static (i.e., $\omega = 0$) stiffness matrix (whose units are given in kN and mm) and loading vector for the particular case of dense sand [$k_S = 0.012\,\text{kN/mm}^2$ and $k_G = 0$] are:

$$K = \begin{bmatrix} 34.03 & 2.58 & 15081.83 & -12.45 \\ 2.58 & 39.30 & 903.15 & -5145.75 \\ 15,081.83 & 903.15 & 31,513,789.69 & 942,917.83 \\ -12.45 & -5145.75 & 942,917.83 & 10,807,841.76 \end{bmatrix}, \text{ and } F_{\text{EF}} = \begin{bmatrix} 219.53\,\text{kN} \\ 152.58\,\text{kN} \\ 292,740.02\,\text{kN mm} \\ -95,651.34\,\text{kN mm} \end{bmatrix}.$$

Using Eq. (58), the vertical deflections and bending moments at A and B are as follows:

$$\begin{Bmatrix} \Delta_a \\ \Delta_b \end{Bmatrix} = \begin{Bmatrix} -6.2 \\ -3.5 \end{Bmatrix} \text{mm and } \begin{Bmatrix} M_a \\ M_b \end{Bmatrix} = \begin{Bmatrix} 196,268.4 \\ -77,683.6 \end{Bmatrix} \text{kN mm}.$$

The calculated static stiffness matrix and loading vector for the particular case of dense sand with $k_S = 0.012\,\text{kN/mm}^2$ and $k_G = 5425.19\,\text{kN}$ are:

$$K = \begin{bmatrix} 35.37 & 2.23 & 14,707.43 & 136.60 \\ 2.23 & 40.94 & 391.27 & -4936.76 \\ 14,707.43 & 391.27 & 32,400,215.85 & 889,783.66 \\ 136.60 & -4936.76 & 889,783.66 & 10,907,525.20 \end{bmatrix} \text{ and } F_{\text{EF}} = \begin{bmatrix} 240.20\,\text{kN} \\ 197.12\,\text{kN} \\ 275,183.12\,\text{kN mm} \\ -88,655.01\,\text{kN mm} \end{bmatrix}.$$

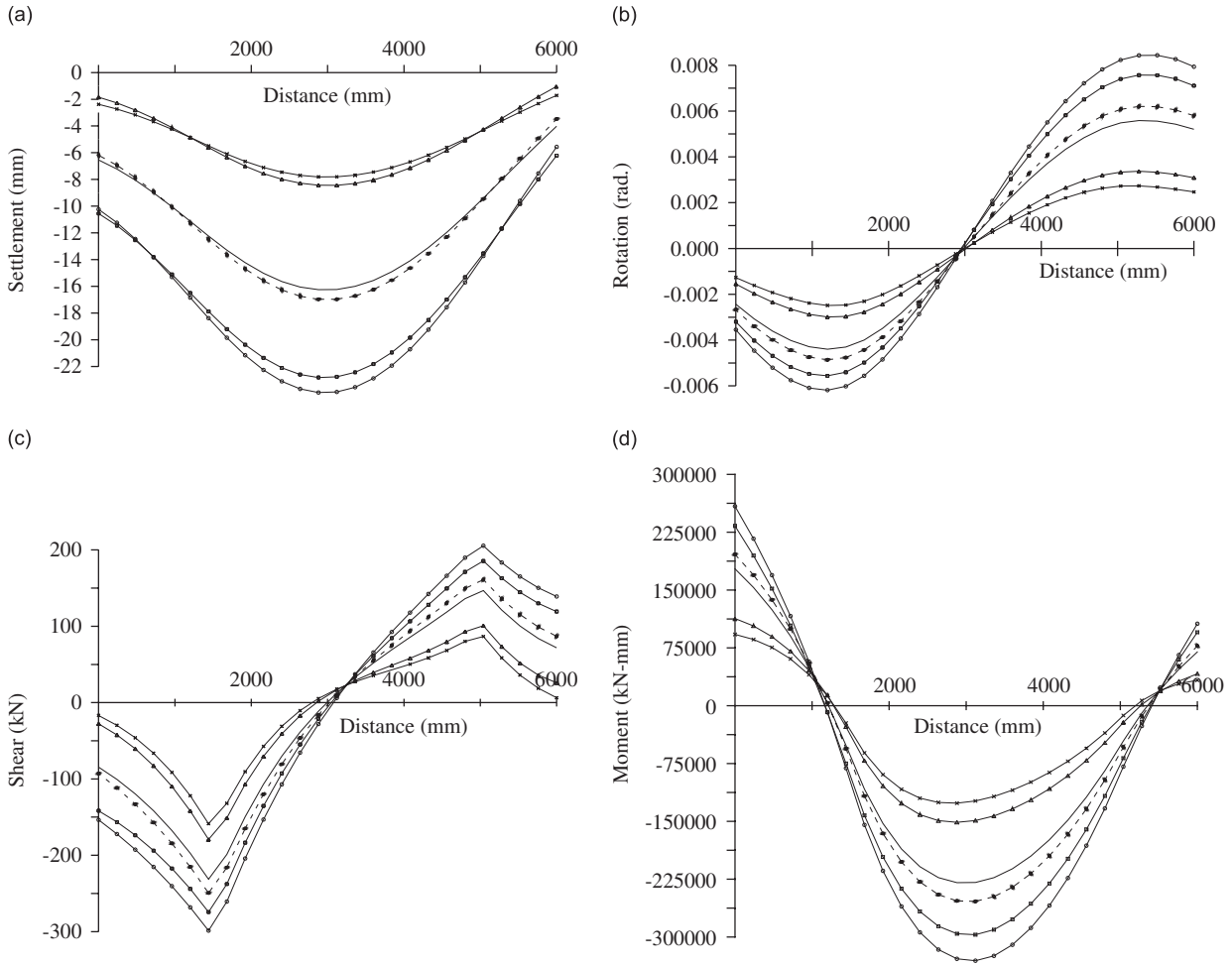

Fig. 5. Example 1: (a) deflection, (b) rotation, (c) shear force, and (d) bending moment. (—×—) Sand and gravel ($k_S = 0.0298\,\text{kN/mm}^2$, $k_G = 14{,}681\,\text{kN}$); (—△—) sand and gravel ($k_S = 0.0298\,\text{kN/mm}^2$, $k_G = 0$); (—) dense sand ($k_S = 0.012\,\text{kN/mm}^2$, $k_G = 5425.19\,\text{kN}$); (– – –) dense sand ($k_S = 0.012\,\text{kN/mm}^2$, $k_G = 0$); (●) dense sand (after Areiza-Hurtado et al. [21]) ($k_S = 0.012\,\text{kN/mm}^2$, $k_G = 0$); (—□—) medium clay ($k_S = 0.0072\,\text{kN/mm}^2$, $k_G = 4989.1\,\text{kN}$); (—○—) medium clay ($k_S = 0.0072\,\text{kN/mm}^2$, $k_G = 0$).

Again, using Eq. (58), the vertical deflections and bending moments at A and B are as follows:

$$\begin{Bmatrix} \Delta_a \\ \Delta_b \end{Bmatrix} = \begin{Bmatrix} -6.5 \\ -4.0 \end{Bmatrix} \text{mm} \quad \text{and} \quad \begin{Bmatrix} M_a \\ M_b \end{Bmatrix} = \begin{Bmatrix} 177,469.72 \\ -69,710.55 \end{Bmatrix} \text{kN mm}.$$

The calculated values for the transverse deflection $Y(x)$, angle of rotation $\Theta(x)$, shear force $V(x)$, and bending moment $M(x)$ along the member are presented and compared with those presented by Areiza-Hurtado et al. [21] in Figs. 5a–d. The proposed dynamic-stiffness matrix and load vector presented above capture the second-order static stiffness matrix and load vector derived by Areiza-Hurtado et al. [21].

Figs. 5a–d also indicate that the elastic response of beam-columns on elastic foundations is strongly affected by the type of soil, and in particular by the magnitude of its first-parameter k_S. The calculated values of the transverse deflections, rotations, shears, and moments along the member are slightly reduced when the magnitude of the second-parameter k_G is increased.

(II) *Free vibration analysis*: The natural frequencies of the beam-column of Fig. 4a can be determined using Eq. (56) by making the determinant of the dynamic-stiffness matrix equal to zero. Table 3 shows the calculated results of the first five natural frequencies (ω) for two cases of elastic (dense sand) foundations. The calculated

Table 3
Example 1: natural frequencies (Hz)

Mode of vibration	Proposed method (dense sand)		SAP 2000 [29]	(a)/(c)
	$k_S = 0.012\,\text{kN/mm}^2$ $k_G = 0$ (a)	$k_S = 0.012\,\text{kN/mm}^2$ $k_G = 5425.19\,\text{kN}$ (b)	$k_S = 0.012\,\text{kN/mm}^2$ $k_G = 0$ (c)	
1	25.64	25.88	25.77	0.9950
2	34.33	35.25	34.84	0.9854
3	54.84	57.06	56.50	0.9706
4	100.02	102.94	104.17	0.9602
5	168.37	171.37	175.44	0.9597

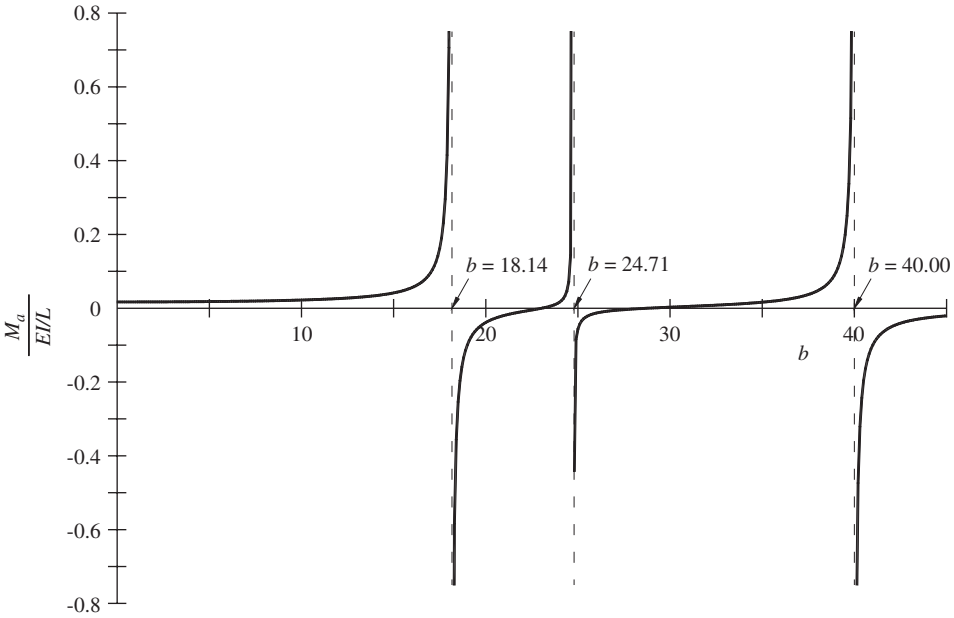

Fig. 6. Example 1: variation of moment at A with the frequency parameter, $b = \omega \Big/ \sqrt{EI/\tilde{m}L^4}$.

results of the particular case when $k_S = 0.012\,\text{kN}$ and $k_G = 0$ are compared with those using the computer program SAP2000 [29] (modeled with 50 segments along the member). It is shown that the proposed method, with just a single segment, compares well with the finite element formulation that generally requires a lot of segments along the member to achieve an acceptable level of accuracy. In addition, most FEM programs like the SAP2000 [29] do not have the capability to simulate the effects of the rotational inertia along the members.

The proposed method not only has the capability to evaluate the effects of the applied frequency on the stiffness matrix, but also on the loading vector. Fig. 6 shows the variation of the moment at A with the applied frequency parameter b for the particular loading case shown in Fig. 4a with foundation properties $k_S = 0.012\,\text{kN}$ and $k_G = 5425.19\,\text{kN/mm}^2$. Notice that the value of the bending moment at end A (M_a) increases as the frequency of the applied load approaches any undamped natural frequency of the beam-column. When resonance conditions are reached, the values of the end moments and forces become infinity.

4.2. Steel frame supported by reinforced-concrete caissons and a beam-on-grade

Consider the plane frame shown in Fig. 7a made up of six members: two reinforced-concrete caissons (EC and FD) rigidly connected by a beam-on-grade (CD) and members AB, CA and DB made of structural steel

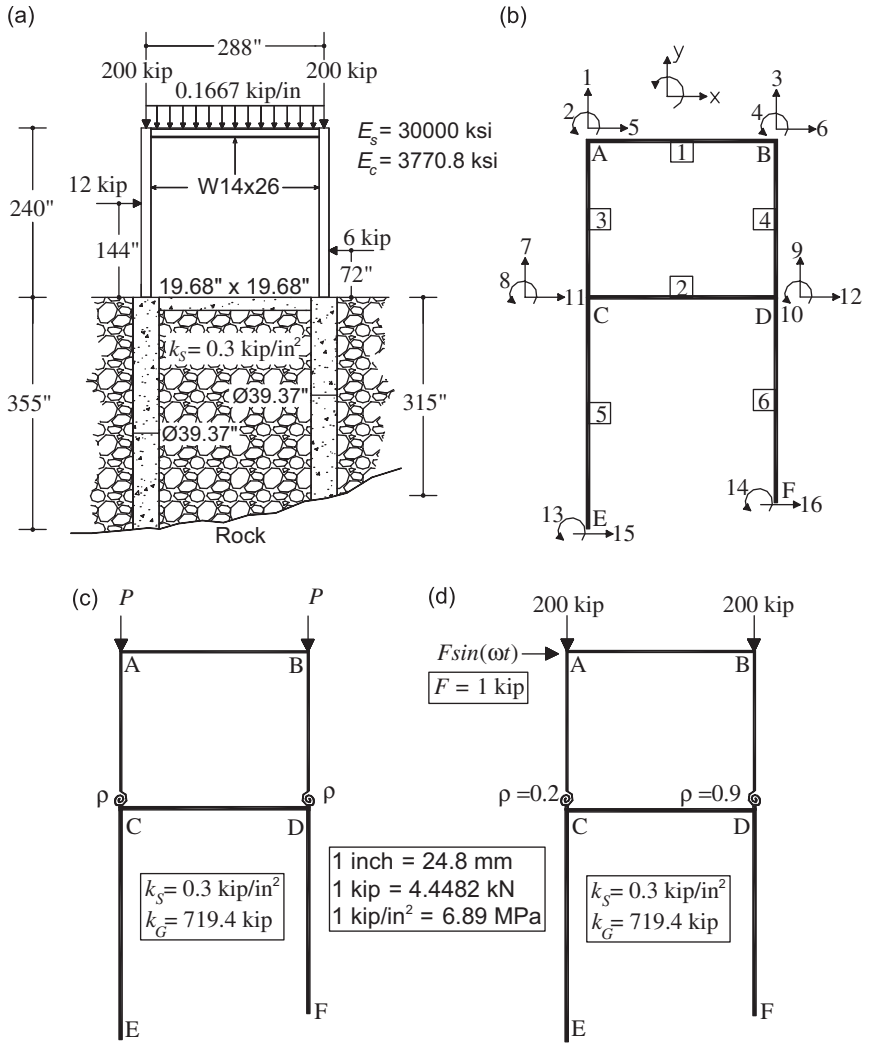

Fig. 7. Plane frame: (a) properties and applied loads; (b) model and degrees of freedom; (c) axial loads (stability analysis); and (d) nodal loads (dynamic analysis).

shape W14 × 26 [with $A_g = 7.69\,\text{in}^2$ (4961 mm^2); $k = 0.46$; $I = 245\,\text{in}^4$ ($101.9767 \times 10^6\,\text{mm}^4$); $E = 30{,}000$ ksi (206,842.72 MPa); $G = 11{,}540$ ksi (79,565.50 MPa); $\bar{m} = 56.32 \times 10^{-7}$ kip-s^2/in^2 (38.86 kg/m)]. The reinforced-concrete members have: $E = 3770.8$ ksi (25,998.75 MPa) and $G = 1640$ ksi (11,307.40 MPa). The beam-on-grade (CD) has a section 19.68 × 19.68 in (500 × 500 mm), $k = 0.83$ and $\bar{m} = 870 \times 10^{-7}$ kip-s^2/in^2 (600 kg/m). Both caissons have a diameter of 39.37 in (1000 mm); $k = 0.90$ and $\bar{m} = 2734.34 \times 10^{-7}$ kip-s^2/in^2 (1886.88 kg/m). Fig. 7b shows the structural model and the degrees of freedom at each joint. The supporting soil properties are $k_S = 0.3\,\text{kip/in}^2$ (2.0684 N/mm^2) and $k_G = 719.4$ kip (3200 kN). Assume that the steel beam-to-column and beam-on-grade-to-caisson connections are rigid (i.e., $\rho = 1$, where ρ is the fixity factor defined previously). However, the steel column-to-caisson connections are semi-rigid as shown by Fig. 7c and d. Determine:

(I) The nodal rotations and displacements caused by the static loads applied as shown in Fig. 7a assuming that the connections at joints A–D are rigid (i.e., $\rho = 1$). Study the effects of the second-parameter of soil k_G (varying its value as 0, 1000, 2000 and 3000 kip). Compare the calculated results for the particular case of $k_G = 0$ with those obtained using the FEM computer program SAP2000 [29];

(II) the variation of the first-mode natural frequency with the magnitude of the applied compressive axial load P (Fig. 7c) for the following values of ρ: 0, 0.25, 0.50, 0.75 and 1.0, respectively, and

(III) the first five natural frequencies of the frame and the variation of the lateral displacement of joint 5 as the frame is subjected to a lateral forced vibration $F\sin(\omega t)$ as shown by Fig. 7d. Compare the calculated frequencies for the particular case of $k_G = 0$ and $\rho = 1$ at connections C and D with those obtained using the FEM computer program SAP2000 [29].

Solution:

In the dynamic analysis of the 2-D frame shown in Fig. 7a the axial translational inertia (along the longitudinal axis) of each member is taken into consideration, and as a consequence, the dynamic-stiffness matrix includes also two axial degrees of freedom (5 and 6) along the local x-axis at A and B, respectively (Fig. 3). Therefore, the complete dynamic-stiffness matrix of each member used in the analysis is as follows:

$$K = \begin{bmatrix} K_{11} & K_{12} & K_{13} & K_{14} & 0 & 0 \\ & K_{22} & K_{23} & K_{24} & 0 & 0 \\ & & K_{33} & K_{34} & 0 & 0 \\ & & & K_{44} & 0 & 0 \\ & \text{Symm.} & & & \dfrac{AE}{L} - \dfrac{\bar{m}L\omega^2}{2} & -\dfrac{AE}{L} \\ & & & & & \dfrac{AE}{L} - \dfrac{\bar{m}L\omega^2}{2} \end{bmatrix}. \tag{67}$$

(I) Nodal rotations and displacements caused by the static loads (Fig. 7a), assuming that the connections at joints A–D are rigid (i.e., $\rho = 1$), are listed in Table 4 (for four values of k_G), as well as the results using the FEM computer program SAP2000 [29] for the particular case of $k_G = 0$. Notice that displacements and rotations of nodes are reduced as the value of k_G is increased, particularly at nodes C–F.

(II) The variations of the first-mode natural frequency with the magnitude of the applied compressive axial load P (Fig. 7c) are shown in Fig. 8 for five different values of ρ (0, 0.25, 0.50, 0.75 and 1.0, respectively). The natural frequencies are determined making the determinant of the dynamic-stiffness matrix of the whole structure equal to zero. The critical axial load (P_{cr}) is found making zero the determinant of the dynamic-stiffness matrix of the structure when $\omega = 0$. The buckling loads are: for $\rho = 0$, $P_{cr} = 216.76$ kip

Table 4
Displacements (in) and rotations (rad) of plane frame (static analysis)

Displacement or rotation	$k_G = 0$ kip (a)	$k_G = 1000$ kip (b)	$k_G = 2000$ kip (c)	$k_G = 3000$ kip (d)	SAP2000 [29], $k_G = 0$ (e)	(a)/(e)
Δ_1	−0.2485	−0.2485	−0.2485	−0.2486	−0.2485	0.9999
θ_2	−0.0067	−0.0067	−0.0067	−0.0066	−0.0067	1.0011
Δ_3	−0.2502	−0.2501	−0.2501	−0.2501	−0.2502	1.0000
θ_4	0.0040	0.0040	0.0040	0.0040	0.0040	0.9984
Δ_5	0.8636	0.8408	0.8245	0.8123	0.8481	1.0182
Δ_6	0.8531	0.8303	0.8140	0.8018	0.8376	1.0185
Δ_7	−0.0169	−0.0169	−0.0169	−0.0170	−0.0169	0.9985
θ_8	−0.0005	−0.0004	−0.0003	−0.0003	−0.0004	1.0642
Δ_9	−0.0157	−0.0157	−0.0156	−0.0156	−0.0157	1.0008
θ_{10}	−0.0006	−0.0005	−0.0004	−0.0004	−0.0005	1.0444
Δ_{11}	0.1117	0.0987	0.0894	0.0825	0.0999	1.1189
Δ_{12}	0.1117	0.0987	0.0894	0.0824	0.0998	1.1189
θ_{13}	−0.0004	−0.0003	−0.0003	−0.0002	−0.0004	1.0492
θ_{14}	−0.0005	−0.0004	−0.0003	−0.0003	−0.0005	1.0361
Δ_{15}	−0.0442	−0.0311	−0.0218	−0.0148	−0.0473	0.9344
Δ_{16}	−0.0543	−0.0391	−0.0284	−0.0203	−0.0593	0.9153

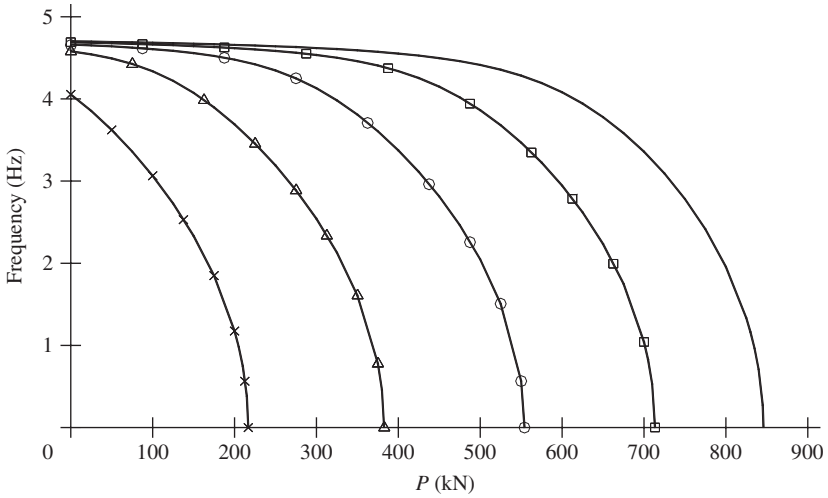

Fig. 8. Example 2: variation of the first-mode frequency with the magnitude of the applied compressive axial load P: (—×—) $\rho = 0$; (—△—) $\rho = 0.25$; (—○—) $\rho = 0.5$; (—□—) $\rho = 0.75$; and (—) $\rho = 1$.

Table 5
Example 2: natural frequencies (Hz)

Mode	Frequency (Hz) (PM[a], assuming $\rho = 1$ at C and D, and $k_G = 0$) (a)	Frequency (Hz) (PM[a], assuming the ρ as shown in Fig. 7d and $k_G = 719.4$ kip) (b)	Frequency (Hz) (using SAP2000 [29], assuming $\rho = 1$ at C and D and $k_G = 0$) (c)	(a)/(c)
1	4.587	4.519	4.638	0.989
2	5.516	5.526	5.599	0.985
3	5.890	5.703	5.981	0.985
4	8.754	7.257	8.780	0.997
5	24.866	25.213	25.063	0.992

[a]PM denotes proposed model.

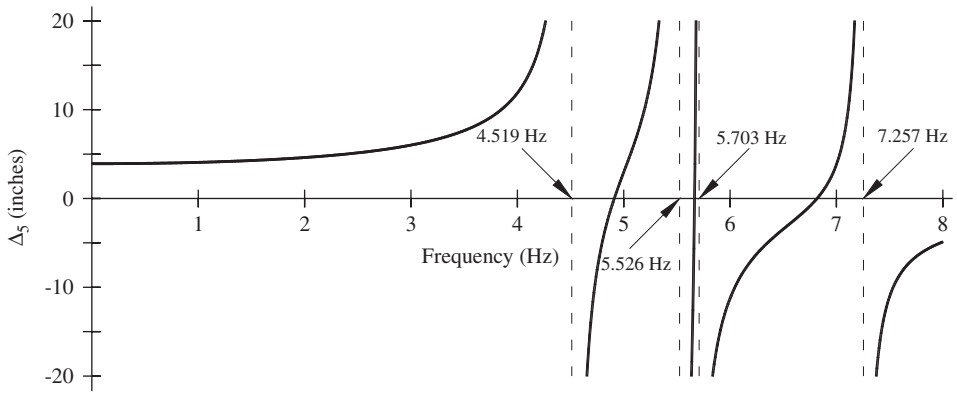

Fig. 9. Example 2: variation of horizontal deflection (Δ_5) with applied frequency (ω).

(964.19 kN); $\rho = 0.25$, $P_{cr} = 382.63$ kip (1702 kN); $\rho = 0.5$, $P_{cr} = 554.07$ kip (2464.6 kN); $\rho = 0.75$, $P_{cr} = 713.48$ kip (3173.7 kN); and for $\rho = 1.0$, $P_{cr} = 845.87$ kip (3762.6 kN).

(III) Notice that: (1) as expected, the degree fixity at the base of the frame has a great effect on the buckling load of the frame; and (2) the applied compressive axial load P reduces the natural frequency of the

frame, particularly at low values of ρ at its base or connection with the caissons. However, this reduction is not substantial for values of $\rho > 0.75$ and with the applied axial load P less than $0.50P_{cr}$.

(IV) The first five natural frequencies of the frame in Fig. 7d are listed in Table 5. The variation of the lateral displacement of joint 5 (Δ_5) with the frequency (ω) as the frame is subjected to the lateral force $F\sin(\omega t)$ is shown in Fig. 9. As expected, Δ_5 becomes infinity as the frequency of the applied force F reaches any of the natural frequencies of the undamped frame (i.e., at resonance). It is important to emphasize two features of the dynamic behavior of this frame: (1) for lower frequencies (lower than 2.5 Hz), small variations of the lateral displacement were computed; and (2) since the first four natural frequencies of the frame are not too far apart from each other, the displacements varies rapidly from $+\infty$ to $-\infty$ as the applied frequency varies from 4 to 8 Hz.

4.3. Free vibration tests of reinforced-concrete cantilever walls

Determine the fundamental natural frequency for a series of R/C structural walls reported by Aristizabal-Ochoa [16] whose properties are listed in Table 6. Also, calculate the first three modes of vibration for specimen F1 and compare the results with those using SAP2000 [29]. The model used for the walls is shown in Fig. 10a. Assume that: Poisson ratio, $\mu = 0.15$; $L = 4.57$ m; $m_b = 1404.51$ kg; and $J_b = 657.93\,\text{kg}\,\text{m}^2$ for all specimens.

Solution:

The structural model and degrees of freedom are shown in Fig. 10(b). Table 7 lists both the measured (experimental) and calculated fundamental frequencies for all eight walls according to: (a) the proposed

Table 6
Example 3: properties of R/C cantilevered walls (after Aristizabal-Ochoa [16])

Specimen	I (m^4)	A_g (m^2)	$\bar{m}$ (kg/m)	k	E (MPa)
F1	0.193	0.359	861.6	0.52	25,424.1
B1	0.139	0.317	760.8	0.58	28,111.2
B2	0.139	0.317	760.8	0.58	28,938
B3	0.139	0.317	760.8	0.58	27,284.4
B4	0.139	0.317	760.8	0.58	28,249
B5	0.139	0.317	760.8	0.58	27,353.3
R1	0.058	0.193	463.2	0.83	27,766.7
R2	0.058	0.193	463.2	0.83	26,802.1

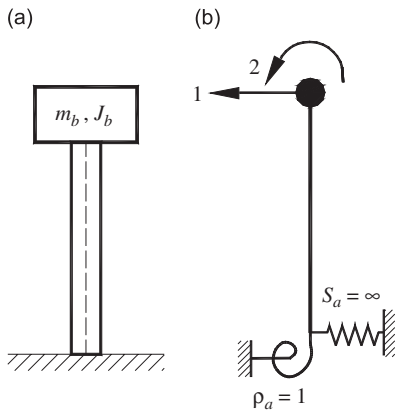

Fig. 10. Example 3: (a) cantilever wall; and (b) structural model and degrees of freedom.

Table 7
Example 3: fundamental frequency (after Aristizabal-Ochoa [16])

Specimen	Fundamental frequency (Hz)				(a)/(b)
	Measured (experimental) (a)	Calculated (proposed method) (b)	Calculated [16] (c)	Calculated [29] (d)	
F1	33.80	33.78	33.90	34.14	1.00
B1	30.00	32.19	32.20	32.46	0.93
B2	29.40	32.66	32.70	32.89	0.90
B3	29.70	31.72	31.70	31.94	0.94
B4	29.20	32.27	32.30	32.47	0.90
B5	30.10	31.76	31.80	32.05	0.95
R1	21.80	23.86	23.80	24.10	0.91
R2	17.80	23.44	23.40	23.64	0.76

Table 8
Example 3: first, second and third natural frequencies of wall F1

Model	Proposed model (including rotational inertia along the wall) (a)	Proposed model (excluding rotational inertia along the wall) (b)	SAP2000 [29] (excludes rotational inertia along the wall) (c)	(a)/(c)	(b)/(c)
1	33.78	34.21	34.25	0.99	1.00
2	141.01	148.63	149.25	0.94	1.00
3	285.45	307.73	312.50	0.91	0.98

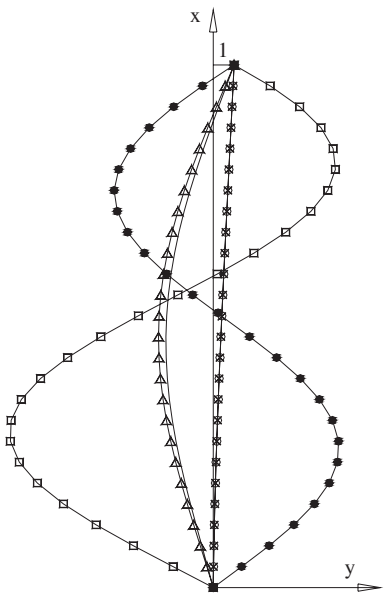

Fig. 11. Example 3: modes of vibration of wall F1: (—o—) first mode, proposed model; (—×—) first mode, SAP2000 [29]; (—△—) second mode, proposed model; (—) second mode, SAP2000 [29]; (—□—) third mode, proposed model; and (—●—) third mode, SAP2000 [29].

method; (b) the method reported by Aristizabal-Ochoa [16]; and (c) the computer program SAP2000 [29] (modeled with 50 segments along the member).

Table 8 shows the first three natural frequencies of specimen F1. As mentioned before, SAP2000 [29] does not have the capability to simulate the effects of rotational inertia along the members, and consequently the

values of the natural frequencies shown in Table 8 (column c) are larger than those obtained with the proposed method including the rotational inertia along the member (column a) and very close to those listed in column b excluding the rotational inertia along the member.

Fig. 11 shows the first-, second- and third-modes of vibration of specimen F1 calculated using the proposed model with and without the effects of the rotational inertia along the wall and those calculated using SAP2000 [29]. These effects are not noticeable in the first mode, but they are in the higher modes. For instance, the node of the second-mode of vibration moves up, the second node of the third-mode disappears, and the amplitudes along the span are larger than those predicted by SAP2000 [29].

5. Summary and conclusions

The dynamic-stiffness matrix and load vector of a Timoshenko beam-column with generalized end conditions and resting on a two-parameter elastic foundation are presented. The proposed model includes the frequency effects on the stiffness matrix and load vector as well as the coupling effects of: (1) bending and shear deformations along the member; (2) translational and rotational lumped masses at both ends; (3) translational and rotational masses uniformly distributed along its span; (4) static axial load (tension or compression) applied at both ends; and (5) shear forces along the span induced by the applied axial load as the beam deforms according to the "modified shear equation" proposed by Timoshenko.

Analytical results indicate that the static, dynamic and stability behavior of framed structures made of beam-columns are highly sensitive to the coupling effects just mentioned. The dynamic-stiffness matrix and load vector are programmed using classic matrix methods to study the static, dynamic, and stability behavior of framed structures made up of beam-columns with semi-rigid end connections and resting on two-parameter elastic foundations.

The proposed model and corresponding dynamic matrix and load vector represent a general approach capable to solve, just by using a single segment per element, the static, dynamic and stability analyses of any elastic framed structure made of prismatic beam-columns with semi-rigid connections. For instance, the static and stability analyses of framed structures under static loads can be carried out by making the problem frequency (or time) independent or simply $\omega = 0$. On the other hand, the dynamic and stability analyses of framed structures under time-dependent loads are carried out including the effects of the imposed frequency ($\omega > 0$) on the dynamic-stiffness matrix and load vector.

The proposed model and corresponding equations represent a general solution to solve the interactions between the aforementioned 19 dimensionless parameters and indices in the static, dynamic and stability analyses of any elastic prismatic beam-column with semi-rigid connections.

Three examples are presented that show the capacities and the validity of the proposed method along with the dynamic-stiffness matrix and loading vector and the obtained results are compared with results from other analytical methods including the finite element method.

Acknowledgements

The research presented in this paper was carried out at the National University of Colombia, School of Mines at Medellín, while the first two authors were members of the Structural Stability Research Group (GES). The authors wish to acknowledge the National University of Colombia (DIME) for providing financial support.

Appendix A. External load expressed in terms of Fourier series

The Fourier series for an arbitrary function $Q(x)$ along the interval $(-L, L)$ is as follows:

$$Q(x) = \frac{a_o}{2} + \sum_{n=1}^{\infty} a_n \cos\left(\frac{n\pi}{L}x\right) + b_n \sin\left(\frac{n\pi}{L}x\right), \tag{A.1}$$

where $a_o = (1/L)\int_{-L}^{L} Q(x)\,\mathrm{d}x$, $a_n = (1/L)\int_{-L}^{L} Q(x)\cos\big((n\pi/L)x\big)\,\mathrm{d}x$, and $b_n = (1/L)\int_{-L}^{L} Q(x)\sin\big((n\pi/L)x\big)\,\mathrm{d}x = 0$.

Notice that if the function $Q(x)$ is symmetric about the origin then $b_n = 0$. The applied transverse load as a function of x and t is

$$q(x,t) = \left[\frac{a_o}{2} + \sum_{n=1}^{\infty} a_n \cos\left(\frac{n\pi}{L}x\right)\right] \sin\, wt, \tag{A.2}$$

where $a_o = (2/L)\int_0^L Q(x)\,\mathrm{d}x$ and $a_n = (2/L)\int_0^L Q(x)\cos\big((n\pi/L)x\big)\,\mathrm{d}x$, or in a dimensionless form:

$$q(\bar{x},t) = \left[\frac{a_o}{2} + \sum_{n=1}^{\infty} a_n \cos(n\pi\bar{x})\right] \sin\, wt, \tag{A.3}$$

where $a_o = 2\int_0^1 Q(\bar{x})\,\mathrm{d}\bar{x}$ and $a_n = 2\int_0^1 Q(\bar{x})\cos(n\pi\bar{x})\,\mathrm{d}\bar{x}$.

For the particular case of a trapezoidal distributed load (dimensionless):

$$Q(\bar{x}) = \begin{cases} 0, & 0 \leqslant \bar{x} < \bar{a}, \\ Q_a + \left(\dfrac{Q_b - Q_a}{\bar{b} - \bar{a}}\right)(\bar{x} - \bar{a}), & \bar{a} \leqslant \bar{x} \leqslant \bar{b}, \\ 0, & \bar{b} < \bar{x} \leqslant 1, \end{cases} \tag{A.4}$$

where $Q_a = Q(\bar{a})$, $Q_b = Q(\bar{b})$, $\bar{a} = a'/L$, and $\bar{b} = b'/L$. Solving the integrals of the Fourier coefficients for the trapezoidal distributed load (A.4):

$$a_o = (Q_a + Q_b)(\bar{b} - \bar{a}) \tag{A.5}$$

and

$$a_n = \frac{2(Q_a - Q_b)}{(n\pi)^2(\bar{b} - \bar{a})}[\cos(n\pi\bar{a}) - \cos(n\pi\bar{b})] + \frac{2}{n\pi}[Q_b \sin(n\pi\bar{b}) - Q_a \sin(n\pi\bar{a})], \tag{A.6}$$

the transverse load can be expressed in dimensionless form as follows:

$$\bar{Q}(\bar{x}) = A_o + \sum_{n=1}^{\infty} A_n \cos(n\pi\bar{x}), \tag{A.7}$$

where

$$A_o = \frac{a_o L}{2A_s G}, \tag{A.8}$$

$$A_n = \frac{a_n L}{A_s G}. \tag{A.9}$$

Eqs. (A.1)–(A.9) can be used to model the following loads: (1) uniformly distributed load making $Q_a = Q_b$; (2) triangular distributed load making $Q_a = 0$ and Q_b arbitrary; (3) concentrated load making $\bar{b} = \bar{a} + \xi$ and $Q_a = Q_b = Q/\xi$ as $\xi \to 0$; and (4) concentrated moment at $\bar{a}$ making $\bar{b} = \bar{a} + \xi$ and $Q_a = -Q_b = 6M/\xi^2$ as $\xi \to 0$.

References

[1] S.P. Timoshenko, J.M. Gere, *Theory of Elastic Stability, Engineering Societies Monographs*, McGraw-Hill Book Company, New York, 1961.
[2] T.W. Thomson, *Theory of Vibration with Applications*, Prentice-Hall, Englewood Cliffs, NJ, 1972.
[3] D.R. Blevins, *Formulas for Natural Frequency and Mode Shape*, Van Nostrand Reinhold Co., New York, 1979.
[4] W. Weaver, S.P. Timoshenko, D.H. Young, *Vibration Problems in Engineering*, fifth ed., Wiley/Interscience, New York, 1990.
[5] R.W. Clough, J. Penzien, *Dynamics of Structures*, McGraw-Hill Book Co., New York, 1993.

[6] S.P. Timoshenko, On the correction for shear of the differential equation for transverse vibrations of prismatic bars, *Philosophical Magazine* 41 (1921) 744–746.
[7] S.P. Timoshenko, On the transverse vibrations of bars of uniform cross-section, *Philosophical Magazine* 43 (1922) 125–131.
[8] F.Y. Cheng, Vibrations of Timoshenko beams and frameworks, *Journal of the Structural Division-ASCE* 96 (3) (1970) 551–571.
[9] F.Y. Cheng, W.H. Tseng, Dynamic matrix of Timoshenko beam columns, *Journal of the Structural Division-ASCE* 99 (3) (1973) 527–549.
[10] F.Y. Cheng, C.P. Pantelides, Dynamic Timoshenko beam-columns on elastic media, *Journal of Structural Engineering-ASCE* 114 (7) (1988) 1524–1550.
[11] K. Morfidis, I.E. Avramidis, Formulation of a generalized beam element on a two-parameter elastic foundation with semi-rigid connections and rigid offsets, *Computers and Structures* (80) (2002) 1919–1934.
[12] K. Morfidis, I.E. Avramidis, Generalized beam-column finite element on two-parameter elastic foundation, *Structural Engineering and Mechanics* 21 (5) (2005) 519–538.
[13] L.E. Goodman, J.G. Sutherland, Discussion of natural frequencies of continuous beams of uniform span length, *Journal of Applied Mechanics-ASME* 18 (1951) 217–218.
[14] T.C. Huang, The effect of rotatory inertia and of shear deformation on the frequency and normal mode equations of uniform beams with simple end conditions, *Journal of Applied Mechanics-ASME* 28 (1961) 579–584.
[15] W.C. Hurty, J.C. Rubenstein, On the effect of rotatory inertia and shear in beam vibration, *Journal of the Franklin Institute* 278 (1964) 124–132.
[16] J.D. Aristizabal-Ochoa, Cracking and shear effects on structural walls, *Journal of Structural Engineering-ASCE* 109 (5) (1983) 1267–1277.
[17] B. Geist, J.R. McLaughlin, Double eigenvalues for the uniform Timoshenko beam, *Applied Mathematics Letters* 10 (1997) 129–134.
[18] B.A.H. Abbas, Vibration of Timoshenko beams with elastically restrained ends, *Journal of Sound and Vibration* 97 (1984) 541–548.
[19] E. Kausel, Nonclassical modes of unrestrained shear beams, *Journal of Engineering Mechanics-ASCE* 133 (6) (2002) 663–667.
[20] J.D. Aristizabal-Ochoa, Timoshenko beam-column with generalized end conditions and non-classical modes of vibration of shear beams, *Journal of Engineering Mechanics-ASCE* 130 (10) (2004) 1151–1159.
[21] M. Areiza-Hurtado, C. Vega-Posada, J.D. Aristizabal-Ochoa, Second-order stiffness matrix and loading vector of a beam-column with semirigid connections on an elastic foundation, *Journal of Engineering Mechanics-ASCE* 131 (7) (2005) 752–762.
[22] M. Hetenyi, *Beams on Elastic Foundation*, The University of Michigan Press, Ann Arbor, MI, 1967.
[23] J.D. Aristizabal-Ochoa, First-and second-order stiffness matrix and load vector of beam columns with semi-rigid connections, *Journal of Structural Engineering-ASCE* 123 (5) (1997) 669–678.
[24] J.D. Aristizabal-Ochoa, Stability and second-order analyses of frames with semi-rigid connections under distributed axial loads, *Journal of Structural Engineering-ASCE* 127 (11) (2001) 1306–1314.
[25] I.A. Karnovsky, O.L. Lebed, *Formulas for Structural Dynamics: Tables, Graphs and Solutions*, McGraw-Hill, New York, 2001.
[26] V.Z. Vlasov, U.N. Leontiev, *Beams, plates, and shells on elastic foundation,* Jerusalem: Israel program for Scientific Translations (Translated from Russian), 1966.
[27] F. Zhaohua, R.D. Cook, Beam elements on two parameter elastic foundation, *Journal of Engineering Mechanics-ASCE* 109 (6) (1983) 1390–1402.
[28] B.M. Das, *Principles of Foundation Engineering*, PWS Kent Publishing Company, Boston, 1999.
[29] SAP2000, version 6.1, *SAP2000 Integrated Finite Element Analysis and Design of Structures*, 1995, Computers and Structures, Inc., Berkeley, CA 94704, USA, 1997.